Efficient Charge Separation in Porphyrin-Fullerene-Ligand Complexes

Tatiana Da Ros,[a] Maurizio Prato,*[a] Dirk M. Guldi,*[b] Marco Ruzzi,[c] and Luigi Pasimeni*[c]

Dedicated to Professor Fred Wudl on the occasion of his 60th birthday

Abstract: Photoprocesses associated with the complexation of a pyridine-functionalized C_{60} fullerene derivative to ruthenium- and zinc-tetraphenylporphyrins (tpp) have been studied by time-resolved optical and transient EPR spectroscopies. It has been found that upon irradiation in toluene, a highly efficient triplet–triplet energy transfer governs the deactivation of the photoexcited [Ru(tpp)], while electron transfer (ET) from the porphyrin to the fullerene prevails in polar solvents. Complexation of [Zn(tpp)] by the fullerene derivative is reversible and, following excitation of the [Zn(tpp)], gives rise to very efficient charge separation. In fluid polar solvents such as THF and benzonitrile, radical-ion pairs (RPs) are generated both by intramolecular ET inside the complex and by intermolecular ET in the uncomplexed form. Charge-separated states have lifetimes of about 10 μs in THF and several hundred of microseconds in benzonitrile at room temperature.

Keywords: electron transfer · EPR spectroscopy · fullerenes · ion pairs · porphyrins

Introduction

The study of the individual steps of natural photosynthesis is a very complicated matter, and their full comprehension is still a formidable task. For example, it is known that in bacterial photosynthetic reaction centers, for which detailed structural information is available, a series of efficient electron-transfer (ET) events occur.[1–3] The long-lived charge-separated species evolve to generate a cross-membrane potential that governs subsequent fundamental biochemical reactions. Owing to the importance and complexity of this phenomenon, suitable simpler models are necessary.[4–8] In this context, photoactive supramolecular systems, in which a donor and an acceptor moiety are noncovalently linked, are particularly appealing.[9–12] In such systems, a rapid photoinduced ET should be followed by a diffusional splitting of the charge-separated radical pair, mimicking a key step in natural photosynthesis. Recently, fullerene C_{60} has emerged as a new three-dimensional acceptor moiety and has been studied under a variety of conditions.[13–17] Driven by an exceptionally low reorganization energy,[18, 19] ET to C_{60} proceeds rapidly relative to comparable two-dimensional electron acceptors. More importantly, this effect leads to a significant decrease in the rate of back electron transfer (BET). In this paper we describe the synthesis and photophysical properties of two fullerene-porphyrin dyads, **1** and **2**, in which the two chromophores are linked together through axial ligation. Zinc- and ruthenium-porphyrin complexes have been investigated and ligation to the porphyrin metal has been ensured using a pyridine-containing fulleropyrrolidine.[20–22]

[a] Prof. M. Prato, Dr. T. Da Ros
Dipartimento di Scienze Farmaceutiche
Università di Trieste, Piazzale Europa 1
34127 Trieste (Italy)
E-mail: prato@univ.trieste.it

[b] Dr. habil. D. M. Guldi
Radiation Laboratory, University of Notre Dame
Notre Dame, IN 46556 (USA)

[c] Prof. L. Pasimeni, Dr. M. Ruzzi
Dipartimento di Chimica Fisica
Università di Padova, Via Loredan 2 (Italy)

Results and Discussion

Ligand **3** (Scheme 1) was prepared by azomethine ylide cycloaddition to C_{60},[23, 24] by using sarcosine and 4-pyridine aldehyde as the starting materials.[25] The [Ru(tpp)(CO)C_{60}] complex **1** was prepared by reaction of commercially available [Ru(tpp)(CO)ROH] **4** and pyridine **3**. [Ru(tpp)(CO)ROH] **4** has one alcohol molecule very weakly bound to the metal. In the presence of a stronger ligand, such as pyridine, the alcohol is immediately displaced.[26] Thus the reaction between **3** and **4** takes place instantaneously at room temperature, affording the new complex **1** in quantitative yield (Scheme 1). The formation of the complex is easily followed by ^{1}H NMR spectroscopy: the pyridine protons adjacent to nitrogen are

0947-6539/01/0704-0816 $ 17.50+.50/0

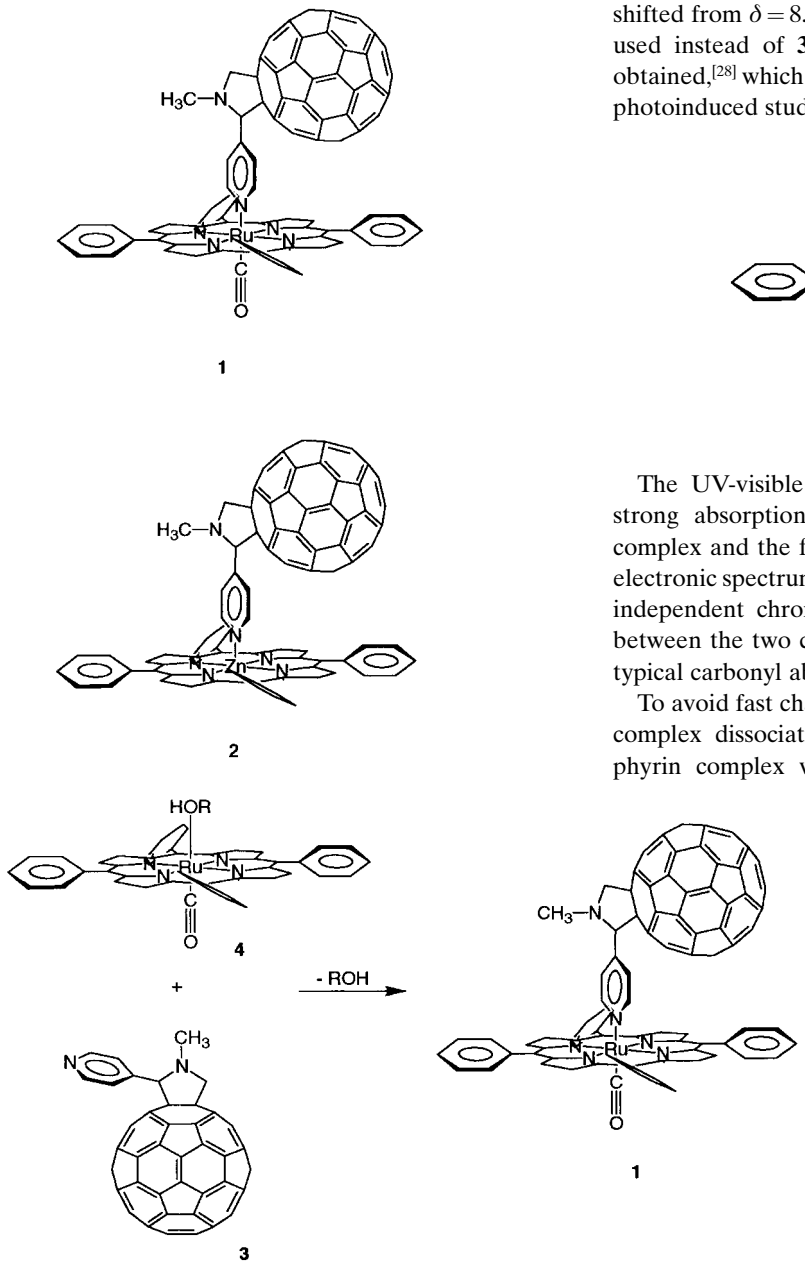

Scheme 1. Reaction scheme for the formation of **1**.

Abstract in Italian: *In questo lavoro viene riportato il comportamento fotoindotto di due diadi, ottenute attraverso coordinazione di un derivato fullerenico contenente un frammento piridinico a una rutenio o a una zinco tetrafenilporfirina. I processi sono stati studiati mediante due diverse spettroscopie risolte nel tempo: ottica ed EPR. Mentre in toluene, in seguito a irraggiamento, si osserva il trasferimento di energia dalla porfirina al fullerene, in solventi più polari prevale il trasferimento elettronico. Nel caso della [Zn(tpp)] dallo stato eccitato si ottiene un'efficiente separazione di carica sia in processi intramolecolari (nella forma complessata) che in processi intermolecolari (nella forma non complessata). Per la [Zn(tpp)], i tempi di vita delle coppie ioniche generate sono notevoli, alcuni microsecondi in THF e diverse centinaia di microsecondi in benzonitrile a temperatura ambiente.*

shifted from $\delta = 8.7$ in **3** to $\delta = 1.5$ in **1**.[27] When pyridine was used instead of **3**, the [Ru(tpp)(CO)py] complex (**5**) was obtained,[28] which was used as a reference in ground state and photoinduced studies.

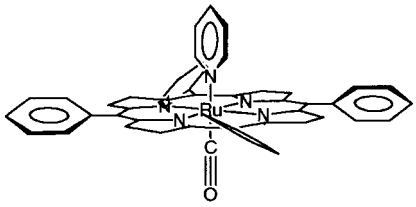

5

The UV-visible absorption spectrum of dyad **1** displays strong absorptions due to both the porphyrin-ruthenium complex and the fullerene moieties. As a matter of fact, the electronic spectrum of **1** is the virtual superposition of the two independent chromophores, with no detectable interaction between the two centers (Figure 1). The IR spectrum shows typical carbonyl absorption at 1962 cm^{-1}.

To avoid fast charge recombination by taking advantage of complex dissociation (vide infra), a weaker fullerene-porphyrin complex was also investigated. The square-planar compound [Zn(tpp)] forms only weak complexes with pyridine-based ligands. Typically, these complexes have equilibrium constants (K) on the order of 5000 M^{-1}.[21] The ligand coordination to the metal in these complexes has been rationalized in terms of π back-bonding, which strengthens the Ru–N coordination bond. In the case of [Zn(tpp)], the π back-bonding is absent and the complexation is only governed by the much weaker σ bonding.

With the objective of probing the complexation of the fullerene ligand, the absorption spectrum of [Zn(tpp)] (**6**) was measured with different concentrations of **3**. In toluene, for example, the two *Q*-band transitions at 549 nm and 589 nm, upon addition of variable amounts of the fullerene ligand, undergo a noticeable red-shift to 552 nm and 598 nm, respectively. Also the Soret band is affected, but gives rise to a less relevant shift. Figure 2 shows the interesting area of the *Q* band of **6** at various concentrations of fullerene **3**. Because of the absorption of compound **3** in the 550–650 nm region, titration of the complex formation is made difficult. Figure 2 (top) shows the uncorrected titration and also the absorption of the fullerene ligand at the same concentration. Subtracting the fullerene absorption produces the spectrum shown in Figure 2 (bottom). Two isosbestic points are now evident at 587 and 557 nm (Figure 2 bottom), for which an equilibrium constant of 5900 M^{-1} was derived. In contrast, a similar addition of a

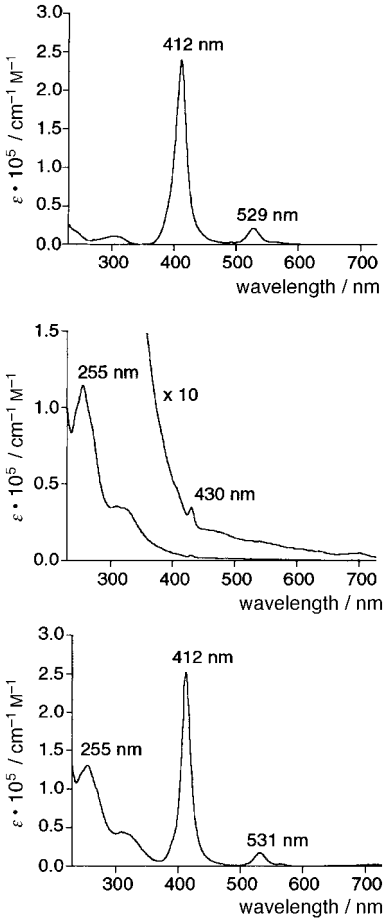

Figure 1. UV/Vis absorption spectra of [Ru(tpp)(CO)py] (**5**) (3.5×10^{-6} M, top), C_{60} derivative **3** (1×10^{-5} M, middle), and complex **1** (2.5×10^{-6} M, bottom) in DCM.

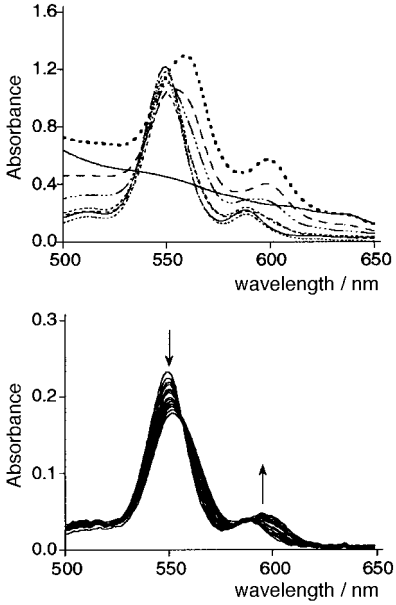

Figure 2. Top: Absorption spectra of [Zn(tpp)] (**6**, 5×10^{-5} M) with and without fullerene ligand **3** (from 1×10^{-5} M to 5×10^{-4} M). Solid line represents the absorption of pure ligand **3** at 5×10^{-5} M concentration. Bottom: Corrected absorption spectrum of [Zn(tpp)] (**6**, 1×10^{-5} M) in the presence of fullerene ligand **3** by using the corresponding pure fullerene **3** solutions at the same concentrations as reference samples.

noncomplexing fullerene derivative (e.g., a dicarbetoxymethanofullerene or *N*-methylfulleropyrrolidine) does not affect the singlet ground-state absorption of the porphyrin and the spectral features of the fullerene derivative and [Zn(tpp)] become virtually superimposable. This leads us to conclude that complexation in **2** occurs through the pyridine nitrogen at an axial coordination site of [Zn(tpp)] with, for example, the unoccupied d_{z^2} orbitals. In the more polar and coordinating solvents such as THF and benzonitrile, no dependence of the spectral features of [Zn(tpp)] on the fullerene **3** concentrations was observed; this indicates a competition in the coordination of Zn between the fullerene pyridine and the solvent.

Semiempirical (PM3) minimization gave an edge-to-edge distance of 4.5 Å between the chromophores or a center-to-center distance of 9.5 Å in system **2**.

Ruthenium-porphyrin optical spectra: Emission yields of the ^{3}*($\pi-\pi$*)[Ru(tpp)] chromophore in complex **1** in various aerated solvents were compared with those of the model [Ru(tpp)(CO)py] (**5**).[28] In general, the emission of the photoexcited chromophore in **1** is noticeably quenched in any of the tested solvents (Table 1). However, a detailed analysis of the solvent dependence reveals a surprising trend. While the porphyrin emission in nonpolar toluene is quenched by nearly 99 and 90% in deareated and aerated solutions of **5**, respectively, the corresponding emission in benzonitrile, a solvent of a much higher dielectric constant ($\varepsilon=25.9$), gives rise to a remarkable increase of the emission yield (Figure 3). The Born formula predicts a strong impact of the solvent polarity on the driving force ($-\Delta G^\circ$) for an intramolecular ET reaction.[29] In contrast to the observed solvent dependence, the exothermic nature of ($-\Delta G^\circ$) is expected to increase as the solvent dielectric constant increases. This may indicate a different quenching mechanism of photoexcited **1** in the two different solvents.

Table 1. Relative emission yields and lifetimes for [Ru(tpp)(CO)py] (**5**) and [Ru(tpp)(CO)C_{60}] (**1**) in solution at room temperature.

Solvent	Conditions	**5**	**1**
toluene ($\varepsilon=2.39$)	oxygen	11	1.1 (85 ps)
	nitrogen	94	1.3
THF ($\varepsilon=7.6$)	oxygen	14	2.7 (460 ps)
	nitrogen	100	17
DCM ($\varepsilon=10.19$)	oxygen	13	1.6 (511 ps)
	nitrogen	91	1.6
benzonitrile ($\varepsilon=25.9$)	oxygen	14	2.8 (404 ps)
	nitrogen	98	24

Furthermore, a red-shift of the emission is noted in going from toluene to benzonitrile, which may be attributed to a more polar surrounding leading to larger Stokes shifts. However, we cannot rule out that a partial change of axial ligation may have taken place, that is, substitution of some of the metalloporphyrins axial ligands.

To follow up on this argument, we complemented the emission experiments of **1** and **5** with measurements in dichloromethane (DCM) and THF. In particular, DCM was chosen because its moderate polarity makes it possible to

0947-6539/01/0704-0818 $ 17.50+.50/0 *Chem. Eur. J.* **2001**, *7*, No. 4

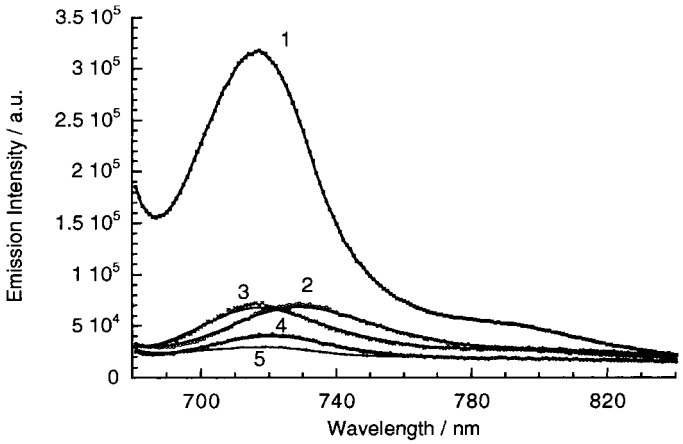

Figure 3. Fluorescence spectra ($\lambda_{exc} = 532$ nm) of solutions of [Ru(tpp)(CO)py] (**5**) in toluene (1) and of [Ru(tpp)(CO)C_{60}] (**1**) (2×10^{-5} M) in benzonitrile (2), THF (3), DCM (4), and toluene (5) at room temperature.

increase the driving force ($-\Delta G^{\circ}$) for an intramolecular ET reaction relative to toluene. At the same time, the insignificant coordinating character of DCM preserves the coordination of the fullerene ligand. Indeed, the porphyrin emission is subject to a marked reactivation relative to the toluene case; this supports the view of a different quenching mechanism. In contrast THF is known to be a coordinating medium, as is benzonitrile. Thus it is not surprising that the emission of **5** in THF was found to be similarly strong to that in benzonitrile.

In cases where the solvent molecules (i.e., THF and benzonitrile) may actually displace the fullerene ligand from the ruthenium porphyrin, omitting oxygen from the solutions is expected to have a profound effect on the porphyrin emission. While in toluene and DCM the emission intensity remains virtually unchanged upon substituting oxygen with nitrogen, in THF and benzonitrile a nearly ten-fold increase in emission was registered. It should be noted that, in comparison to a deoxygenated solution of **5**, the emission of **1** is, however, still noticeably quenched.

In order to shed further light into the deactivation processes and, more fundamentally, to characterize the transient intermediates evolving from the supposedly intramolecular dynamics we probed reference porphyrin **5** and dyad **1** in transient spectroscopy. In particular, the transient differential absorption changes following either a 18 ps or 6 ns laser pulse (both at 532 nm) should ensure the exclusive formation of the photoexcited chromophore, $^{*}(\pi-\pi^{*})$[Ru(tpp)(CO)py], allowing us to measure its lifetime and, in the case of dyad **1**, to visualize the nature and kinetics of the intramolecular-transfer reaction.

In the case of the porphyrin reference **5** excitation leads to the instantaneous bleaching of the *Q*-band absorption centered around 535 and 565 nm. The wavelength region above 600 nm is, on the other hand, governed by the strong absorptions of the excited state (not shown). In this context, it should be mentioned that on the monitored timescale, 50–4000 ps, the generated species is the triplet excited state, $^{3}*(\pi-\pi^{*})$[Ru(tpp)(CO)py], rather than the initially formed and very short-lived singlet excited state, $^{1}*(\pi-\pi^{*})$-[Ru(tpp)(CO)py] ($\tau < 35$ ps) [Eq. (1)].[28] Coordination of the ruthenium by the H_2TPP macrocycle in combination

$$[\mathrm{Ru(tpp)(CO)py}] \xrightarrow{h\nu} {}^{1*}(\pi-\pi^{*})[\mathrm{Ru(tpp)(CO)py}] \xrightarrow{\mathrm{ISC}} {}^{3*}(\pi-\pi^{*})[\mathrm{Ru(tpp)(CO)py}] \quad (1)$$

with the axial ligand (e.g., carbonyl group) has been proposed to be the key step for the rapid intersystem crossing (ISC) of the photoexcited ruthenium-porphyrin complex. Extension of the monitored timescale to the nano-/microsecond time regime allowed us to determine a lifetime of 30 μs for the triplet excited state, which is in good agreement with previously published values.[30]

A similar excitation of the porphyrin antenna is noticed in picosecond-resolved experiments carried out with dyad **1**, by employing a 532 nm laser pulse. In toluene, the characteristic $^{3}*(\pi-\pi^{*})$[Ru(tpp)] absorption transforms rapidly into a broadly absorbing species with a lifetime of 85 ps. The spectrum of the latter is displayed in Figure 4 showing a clear

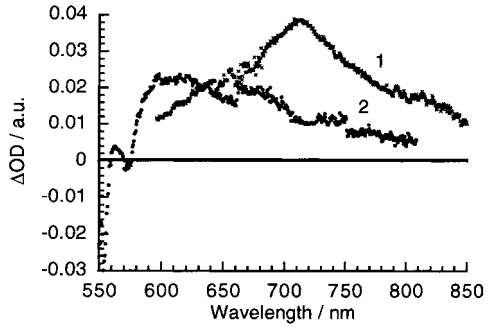

Figure 4. Time-resolved difference absorption spectra of [Ru(tpp)(CO)C_{60}] (**1**) (2.0×10^{-5} M) recorded 200 ps after excitation (532 nm) in oxygen free toluene (1) and 600 ps after excitation (532 nm) in oxygen free benzonitrile (2).

maximum around 710 nm, followed by an energetically lower lying shoulder (820 nm). These features remarkably resemble the triplet excited state of the fullerene core,[31] and suggest an intramolecular energy transfer to the long-lived and highly reactive fullerene triplet state, as shown in Equation (2).

$$^{3}*(\pi-\pi^{*})[\mathrm{Ru(tpp)(CO)C_{60}}] \longrightarrow [\mathrm{Ru(tpp)(CO)}{}^{3}*(\mathrm{C_{60}})] \quad (2)$$

By probing a similar solution in nanosecond experiments the determination of the lifetime and also the quantum yield of the fullerene triplet was achieved. Relative to the non-coordinated fullerene ligand **3**, which served as an internal standard ($\Phi = 0.96$), the photoexcited dyad gave rise to a somewhat smaller triplet quantum yield ($\Phi = 0.65$). In addition, a lifetime of 43 μs, also similar to a directly excited fullerene, further confirms the energy-transfer route. The efficiency observed relates well with the short separation between the two moieties (edge-to-edge distance of 4.5 Å), for which a triplet-triplet energy transfer is expected to be most effective.

As stated above, the emission quenching in benzonitrile follows a surprising trend. Pico-/nanosecond experiments were performed in benzonitrile to relate them to those performed in toluene. The differential absorption changes

recorded immediately after the 18 ps laser pulse (532 nm) are superimposable on those described above: bleaching of the *Q*-band absorption and broad absorption greater than 600 nm are indicative of $^{3}*(\pi-\pi^{*})$[Ru(tpp)(CO)C_{60}]. In line with the emission studies, the excited porphyrin decays with a lifetime of 404 ps and, accordingly, noticeably slower than in toluene. The transient absorption changes in the monitored wavelength region are nonetheless distinctly different from the fullerene triplet state, lacking the characteristic maximum in the visible region at 710 nm (see Figure 4). In contrast, the differential absorption changes show, besides bleaching at 550 nm, a set of new peaks at 565, 610, and 670 nm.

To characterize these transient absorption changes, a complementary pulse radiolytical oxidation experiment of [Ru(tpp)(CO)py] (**5**) in oxygenated DCM solutions was carried out. The resulting radicals, such as $^{\bullet}OCHCl_2$ and $^{\bullet}OCH_2Cl$, are fairly oxidative species[32] and provide the means for oxidation of the ruthenium-porphyrin complex ($E_{1/2}=+0.81$ V versus SCE). Under aerobic conditions [Eq. (3)] pulse radiolysis of the tested [Ru(tpp)] led to a

$$[Ru(tpp)(CO)py]+ {}^{\bullet}OCHCl_2/{}^{\bullet}OCH_2Cl \longrightarrow [Ru(tpp^{\bullet+})(CO)py] \quad (3)$$

differential absorption spectrum, recorded 100 μs after the electron pulse, with intense ground state bleaching in the region corresponding to the *Q* band and broad absorptions in the 550–750 nm wavelength region. It is well documented that ligand centered oxidation of porphyrins gives rise to a broad absorption in the red region (700–840 nm).[33] In contrast, changes in the redox state of the metal in a metalloporphyrin are known to result in minor shifts of the Soret and *Q* bands without strong absorption in the red.[33] On the basis of this precedent, the broad absorption observed upon radiolysis of [Ru(tpp)(CO)py] is ascribed to an oxidation process that occurs on the TPP ligand, yielding the π-radical cation [Eq. (3)].

This π-radical cation absorption is virtually superimposable with those transient changes developing during the picosecond experiments in benzonitrile. Based on this spectral reminiscence we postulate the photoinduced ET mechanism shown in Equation (4).

$$^{3}*(\pi-\pi^{*})[Ru(tpp)(CO)C_{60}] \longrightarrow [Ru(tpp^{\bullet+})(CO)(C_{60}{}^{\bullet-})] \quad (4)$$

The difference in reactivity, namely, energy versus electron transfer, can be best interpreted by calculating the driving force ($-\Delta G^{\circ}$) for an ET mechanism in the two different solvents by employing the dielectric continuum model. This model handles the charge-separated radical pair as two spherical ions separated by a distance (R), submerged into a solvent of a static dielectric constant (ε).[29, 34] The energy level of the [Ru(tpp$^{\bullet+}$)(CO)(C$_{60}^{\bullet-}$)] radical pair is at 1.59 eV and 1.02 eV in toluene and benzonitrile, respectively. In comparison, the energy of the fullerene triplet (1.50 eV)[35] is nearly solvent independent, revealing that in toluene an energy-transfer mechanism evolving from the $^{3}*(\pi-\pi^{*})$[Ru(tpp)] (1.73 eV) is the thermodynamically more favorable process. On the other hand, in benzonitrile $-\Delta G^{\circ}$ appears to be reasonably large (−0.71 eV) and more importantly, substantially greater than $-\Delta G^{\circ}$ for a possible energy transfer (−0.23 eV) activating the ET route. It should be noted that both electron- and energy-transfer processes are very likely to be in the normal region of the Marcus curve.

A closer look at the diagnostic NIR region for the fullerene π-radical anion in Figure 5 yielded support, for example, a distinct maximum at 1010 nm, for the photoinduced generation of a charge-separated radical pair,

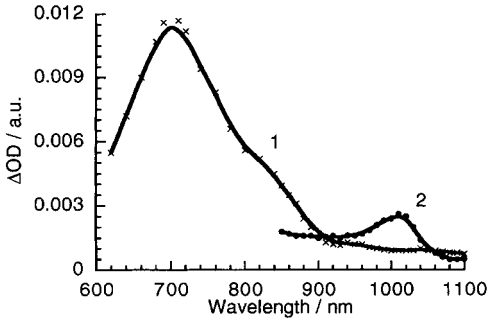

Figure 5. Transient absorption spectrum recorded after 50 ns upon flash photolysis of 2.5×10^{-5} M [Ru(tpp)(CO)C_{60}] (**1**) at 532 nm in deoxygenated toluene (1), and benzonitrile (2).

[Ru(tpp$^{\bullet+}$)(CO)(C$_{60}^{\bullet-}$)]. The π-radical anion absorption is particularly stable and decays on a timescale of about 50 μs. This lifetime is remarkable, since similarly spaced donor–acceptor systems, but which are covalently linked at the *meso*-position of the macrocycle, are subject to an intramolecular BET typically on the order of a few nanoseconds.[36, 37] However, the currently investigated donor–acceptor system differs in that the weak nature of the Ru–N coordination bond in principle enables bond detachment. This has been demonstrated in some earlier work on various [Ru(tpp)py] complexes with dissociation rates of up 2.0×10^{4} s^{-1}.[38]

Complementary measurements in the visible region, which is expected to be governed by the strong metalloporphyrin π-radical cation absorption (550–750 nm), reveals the spectral signature of a porphyrin ligand that has undergone one-electron oxidation as well as similar kinetics, further substantiatiating the long-lived and, presumably, separated radical pair [Eq. (5)].

$$[Ru(tpp^{\bullet+})(CO)(C_{60}{}^{\bullet-})] \longrightarrow [Ru(tpp^{\bullet+})(CO)]+(C_{60}{}^{\bullet-}) \quad (5)$$

The quantum yield for the dissociated free [Ru(tpp$^{\bullet+}$)(CO)(C$_{60}^{\bullet-}$)] couple is 0.1, as measured by the comparative technique. Furthermore, the lifetime of this couple is strongly affected by the dyad concentration. Typically, lifetimes (best fit to a single exponential decay) are on the order of 28.6, 57.9, and 92.5 μs at complex concentrations of 1.0×10^{-4} M, 7.5×10^{-5} M, and 5.0×10^{-5} M, respectively. This dependence clearly points to a charge recombination mechanism that follows second-order kinetics, probably through reassociation of the [Ru(tpp)(CO)C_{60}] complex. In this context it is interesting to note that the absorption spectra of **1** in benzonitrile, before and after

0947-6539/01/0704-0820 $ 17.50+.50/0 *Chem. Eur. J.* **2001**, *7*, No. 4

excitation, were absolutely identical and were also an excellent match to those of **1** in DCM and toluene.

After investigating the two "extreme" (with regard to their dielectric constants) solvents, it seemed to be important to study a solution of dyad **1** in DCM in time-resolved flash photolysis experiments. Despite the unmistakable occurrence of an ET, as evidenced by the formation of the $[Ru(tpp^{\bullet+})(CO)(C_{60}^{\bullet-})]$ pair with a time constant of 511 ps, DCM is insufficient to promote cleavage of the Ru–N coordination bond after the ET event. In particular, a lifetime of < 4 ns, which was derived from the picosecond experiments, suggests that a fast charge recombination prevails over the cleavage of the Ru–N coordination bond. This is in line with the complementary nanosecond experiments, which did not provide any spectral evidence for a charge-separated radical pair. This can be rationalized in terms of the thermodynamic driving force being more exothermic in benzonitrile ($\Delta G^\circ = -0.71$ eV) than in DCM ($\Delta G^\circ = -0.41$ eV).

Ruthenium-porphyrin EPR spectra: Figure 6 shows the EPR spectrum of dyad **1** in toluene matrix recorded at 120 K after illumination of the sample with a 580 nm laser pulse. For comparison we included the computer-simulated spectrum,

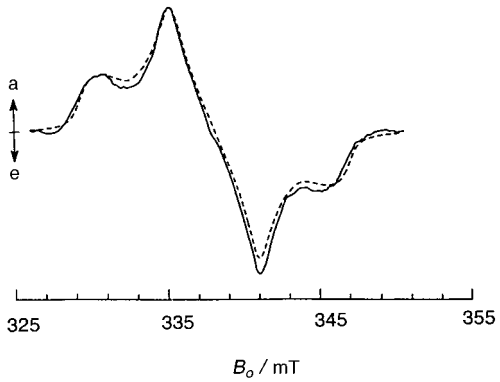

Figure 6. Experimental (solid line) and calculated (dashed line) EPR spectra of dyad **1** detected 0.4 μs after the laser pulse at 120 K in glassy toluene. ZFS parameters of $D = -8.85$ mT and $E = -1.05$ mT, and population ratio $(p_x - p_z)/(p_y - p_z) = 2.36$ ($p_x, p_y > p_z$) were used for fitting. Positive and negative signals indicate absorptive (a) and emissive (e) polarizations.

which was obtained according to a reported procedure.[39] In agreement with the optical results (see above) and based on the zero-field splitting (ZFS) values and the spin-polarization pattern, the spectrum is attributed to the triplet excited state of the fullerene.[40] Following the initial excitation event, a rapid intersystem crossing (ISC) into the corresponding triplet states [^{3}(D*–A) for TPP and ^{3}(D–A*)] for fullerene occurs, with k_{ISC} rate constants.

That only the EPR spectrum of the fullerene triplet was detected suggests that efficient energy transfer from the porphyrin to the fullerene prevails in dyad **1**. The buildup of the transient signal is, however, too rapid with regard to our instrumental time resolution (~ 150 ns). The spin-polarization pattern of the fullerene EPR spectrum is indicative of a singlet excited-state precursor. On the other hand, the lack of the EPR spectrum of the TPP triplet would point to an energy-transfer mechanism.

To unravel the spin multiplicity of the precursor state we examined the spin polarization of the acceptor molecule (fullerene) in detail. Since the spin angular momentum is conserved during a triplet–triplet energy transfer, if the transferred polarization pattern evolves from the TPP triplet, the relative populations of the triplet acceptor sublevels should be proportional to the squares of the projection of the donor principal magnetic axes on the acceptor magnetic axes.[41–43] Spin polarization is, however, not known for the triplet of [Ru(tpp)(CO)py] (**5**) in a toluene glassy solution, and we were not able to detect this species. Thus, energy transfer from the photoexcited triplet state of the porphyrin moiety to the fullerene triplet state, as found in the transient absorption measurements (see above) cannot be confirmed by the TREPR measurements. In a more polar solvent like DCE, we found no evidence of a charge-separated state. It is likely that the short lifetime may prevent detection of the EPR signal. In fact, the lifetime of around 4 ns of the radical pair in a similar solvent (DCM) was obtained by optical methods (see above).

Zinc-porphyrin optical spectra: [Zn(tpp)] displays a high-lying (2.06 eV) and, in contrast to [Ru(tpp)(CO)py] (**5**), a long-lived singlet excited state.[44] Furthermore, based on the strong fluorescence of ^{1}*(π–π*)[Zn(tpp)] ($\Phi = 0.04$), the emission of [Zn(tpp)] can be conveniently employed as a sensitive probe for dynamic and static excited state quenching. For example, solutions of [Zn(tpp)] (**6**; 1.0×10^{-5} M) in toluene and DCM in the presence of **3** (1.3×10^{-5} M) had significantly smaller quantum yields with Φ of 0.0156 and 0.0152, respectively. To further quantify a possible intramolecular deactivation process, a detailed investigation was necessary. Therefore, the steady state emission of the singlet excited metalloporphyrin **6**, ^{1}*(π–π*)[Zn(tpp)], was recorded as a function of fullerene ligand **3**. Figure 7 compares the

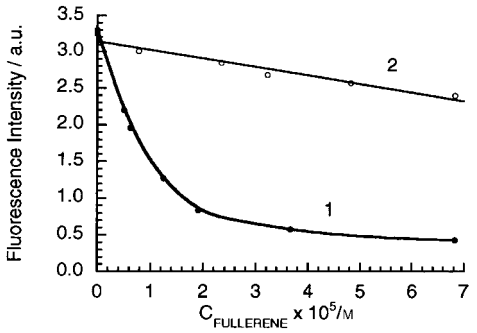

Figure 7. Emission yields of [Zn(tpp)] (**6**, 1.0×10^{-5} M) in deoxygenated toluene solutions in the presence of variable concentrations of fullerene ligand **3** (1) and methanofullerene (2).

dependence for two solutions of [Zn(tpp)] in toluene on fullerene concentration, one with variable concentrations of fullerene ligand **3** and a second one with various quantities of dicarbethoxymethanofullerene. In weakly coordinating solvents, such as toluene and DCM, the emission yields show strong decrements with increasing fullerene concentration.

This leads to the assumption that the $^1*(\pi-\pi^*)$[Zn(tpp)] state is subject to excited state quenching by the electron accepting fullerene moiety, through the possible participation of electron transfer [Eq. (6)]. The intramolecular dynamics of the

$$^1*(\pi-\pi^*)[Zn(tpp)C_{60}] \longrightarrow [Zn(tpp^{\bullet+})(C_{60}^{\bullet-})] \quad (6)$$

resulting dyad **2** in toluene ($5.5\times10^9\,s^{-1}$) and DCM ($7.1\times10^9\,s^{-1}$) were determined by extrapolation of the quenching correlation at high fullerene concentrations to ensure complete complexation conditions (>95%). In light of the strong interactions noticed between the two redox-active moieties, it is feasible to assume that the pyridine-fullerene ligand may indeed coordinate to the metal and accelerate the quenching step.

To prove this hypothesis, a fluorescence experiment was performed by freezing the equilibrium between the [Zn(tpp)] center and the C_{60} ligand. While the investigated system, composed of **3** (1.0×10^{-5} M) and **6** (5.0×10^{-6} M), shows only a moderate loss of emission (30%) at room temperature, it reveals a quantitative quenching of the $^1*(\pi-\pi^*)$[Zn(tpp)] emission (97%) at liquid nitrogen temperature.

Time-resolved irradiation into the porphyrin *Q*-band absorption (532 nm) yielded the characteristic $^1*(\pi-\pi^*)$-[Zn(tpp)] absorptions. This state decayed, in the absence of any fullerene ligand **3**, with a lifetime of 2.5 ns by internal conversion into the energetically lower lying $^3*(\pi-\pi^*)$-[Zn(tpp)] state (Figure 8a). As a consequence of a systematic addition of fullerene ligand **3** to **6** (5.0×10^{-6} M), the singlet lifetime suffered a substantial shortening. For example, in both toluene (1.24×10^{-5} M (**3**): $k=1.2\times10^9\,s^{-1}$) and DCM (1.18×10^{-5} M (**3**): $k=1.8\times10^9\,s^{-1}$), decay rates were determined that are in fairly good agreement with the emission studies. More importantly, these picosecond studies unequivocally establish that the singlet excited-state absorption transforms into a product with minima at 552 and 590 nm and broad absorption features in the red around 715 nm (Figure 8b). However, these are different from those of the porphyrin and fullerene singlet and triplet excited states.

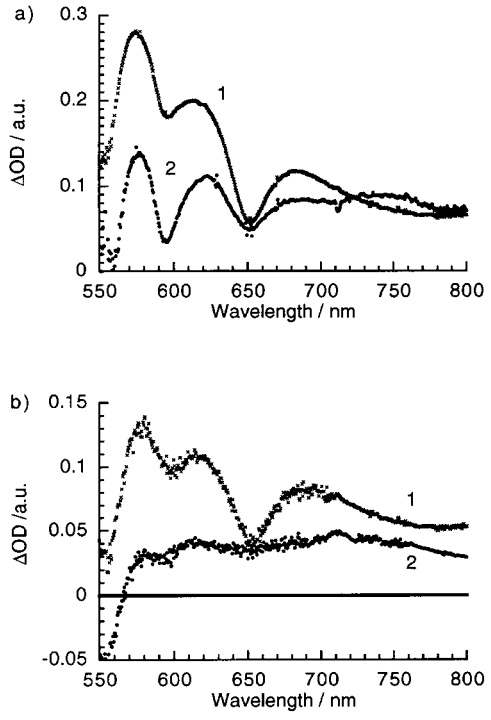

Figure 8. Time-resolved difference absorption spectra of a) [Zn(tpp)] (**6**, 1.0×10^{-5} M) recorded (1) 20 ps after excitation (532 nm) and (2) 4000 ps after excitation (532 nm) oxygen free toluene solution and b) dyad **2** (1.0×10^{-5} M) recorded (1) 20 ps after excitation (532 nm) and (2) 2000 ps after excitation (532 nm) in oxygen free DCM solution.

Differential absorption changes in the visible region, recorded upon nanosecond laser excitation of **2** in DCM [i.e., 5.0×10^{-5} M (**3**) and 5.0×10^{-6} M (**6**)], are shown in Figure 9. They confirm the similarity of the transient product with the one developing through the picosecond timescale.

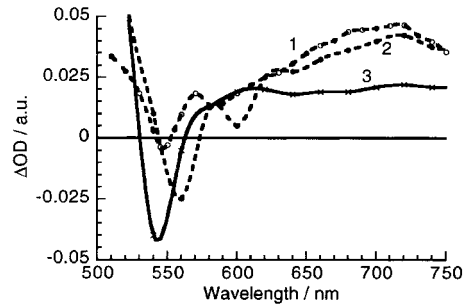

Figure 9. Transient absorption spectrum recorded 50 ns upon flash photolysis (532 nm) of **2** (2.5×10^{-5} M) 1) in deoxygenated dichloromethane and 2) in deoxygenated benzonitrile and [Zn(tpp)] (**6**) (1.0×10^{-5} M) 3) in oxygen-free toluene solution.

The nature of the photoproduct, a charge-separated radical pair ([Zn(tpp$^{\bullet+}$)($C_{60}^{\bullet-}$)]), was successfully identified in DCM by a familiar NIR pattern. Two new transitions at 960 and 1010 nm clearly distinguish the fullerene π-radical anion (similar to the spectral changes depicted in Figure 5). On the other hand, the strong fullerene triplet excited-state absorption around 700 nm, stemming from a possible energy transfer, could not be detected. This leads us to conclude that an intramolecular electron transfer indeed prevails over an energy transfer. Moreover, the absorption characteristics of the radical pair, for example, the porphyrin π-radical cation absorption (600–800 nm) and the fullerene π-radical anion band (1010 nm) were independently confirmed by performing pulse radiolysis. Oxidation [in oxygenated DCM solution; see Eq. (3)] and reduction (in a deoxygenated toluene/acetone/2-propyl alcohol mixture 8:1:1 v/v) experiments were carried out with the [Zn(tpp)] and fullerene ligand centers, respectively.

The diagnostic NIR absorption is also a valuable aid in the determination of the lifetime and quantum yield of the charge-separated radical pair. It is safe to assume that the excess photonic energy of the charge-separated radical pair (~0.9 eV), relative to the precursor $^1*(\pi-\pi^*)$[Zn(tpp)] state (2.06 eV), promotes the bond dissociation and leads to the subsequent separation of the radical pair. A potential complex dissociation at room temperature is further favored by the existing equilibrium. In particular, a half-life of 6 μs observed in DCM represents an efficient retardation of the charge recombination. It should be noted that parallel blank experiments with *N*-methylfulleropyrrolidine and dicarb-

0947-6539/01/0704-0822 $ 17.50+.50/0 *Chem. Eur. J.* **2001**, *7*, No. 4

ethoxymethanofullerene in DCM, despite measurable quenching of the $^{1}*(\pi-\pi^*)$[Zn(tpp)] or $^{3}*(\pi-\pi^*)$[Zn(tpp)] state, did not result in any detectable π-radical cation absorption ([Zn(tpp$^{\bullet+}$)]) or π-radical anion absorption ($C_{60}^{\bullet-}$) throughout the monitored visible and NIR range, respectively. This points to the key function of complex formation (association) as the rate-determining step in the sequence of charge-transfer, charge-separation, and finally charge-recombination processes.

The situation is quite different in a more nucleophilic solvent such as benzonitrile, which based on the cyano-group can be regarded to be a fairly strong ligand. This points to a competition between the solvent molecule (benzonitrile) and the pyridine-based fullerene (**3**) to coordinate with the metal center in **6**. A much higher fluorescence quantum yield ($\Phi = 0.032$) was noted for [Zn(tpp)] **6** (1.0×10^{-5} M) in the presence of **3** (1.3×10^{-5} M) in benzonitrile than in toluene ($\Phi = 0.0156$) and DCM ($\Phi = 0.0152$). Also, the differential absorption changes, particularly in the NIR, reveal the participation of two components in the formation of the fullerene π-radical anion absorption ($C_{60}^{\bullet-}$). The faster process clearly evolves on a subnanosecond timescale, while the slower one occurs on the timescale of several microseconds and probably involves intermolecular quenching of the energetically lower lying $^{3}*(\pi-\pi^*)$[Zn(tpp)] state. The same two-step formation kinetics apply for the visible range, unquestionably yielding [Zn(tpp$^{\bullet+}$)] with minima at 560 and 600 nm concomitant to a broad maximum at 730 nm, shown in Figure 9.

A possible rationale for this observation is based on the interference of the solvent molecule, which competes with the fullerene ligand for the axial coordination sites of the metal center in the rate-determining step enabling the rapid intramolecular ET. In conclusion, while in toluene and DCM intramolecular quenching predominates the deactivation of the $^{1}*(\pi-\pi^*)$[Zn(tpp)], in benzonitrile the two-step formation suggests both intra- and intermolecular ET involving the $^{1}*(\pi-\pi^*)$[Zn(tpp)] state in the former case and the $^{3}*(\pi-\pi^*)$[Zn(tpp)] state in the latter. For the intermolecular reaction in benzonitrile a quenching rate constant of $1.7 \times 10^{10}\,M^{-1}s^{-1}$ was found.

Kinetic analysis of the 1010 nm transient absorption ($C_{60}^{\bullet-}$) gives rise to a remarkable lifetime of the separated radical pair in deoxygenated benzonitrile of several hundred microseconds. The BET obeys second order kinetics with a rate constant of about $1.5 \times 10^{9}\,M^{-1}s^{-1}$.

No significant degradation of either the [Ru(tpp)(CO)py] or [Zn(tpp)C_{60}] complex was measured upon several hundred repetitions of the photoinduced complex dissociation (charge separation) and association (charge recombination) cycles, which result in efficient reconstitution of the ground state complexes.

Finally, a comparison between the quantum yields of the [Ru(tpp$^{\bullet+}$)(CO)($C_{60}^{\bullet-}$)] and [Zn(tpp$^{\bullet+}$)($C_{60}^{\bullet-}$)] couples should be made. We concluded that in the case of [Ru(tpp)] only benzonitrile solutions favor a complex dissociation. This is different for the zinc analogue. In essence, all solvents, except the nonpolar toluene, give appreciable yields of the radical pair, with quantum yields ranging from 0.14 to 0.19 (see Table 2).

Table 2. Quantum yields (Φ) for the formation of a charge-separated radical pair in metalloporphyrin-fullerene dyads as derived from transient absorption measurements.

Solvent	[Ru(tpp)(CO)C_{60}] (**1**)	[Zn(tpp)C_{60}] (**2**)
toluene	energy transfer	0
DCM		0.14
THF	0.015	0.19
benzonitrile	0.10	0.17

Zinc-porphyrin EPR spectra: Based on the results obtained by transient absorption spectroscopy, the time-resolved EPR (TREPR) technique, applied to irradiation of complex **2** in polar solvents should lead to the detection of radical pairs generated in the intermolecular ET (see above). The time domain of our instrumentation, in fact, does not allow the detection of species with lifetimes shorter than 0.1 μs and accordingly only the triplet-born radical pair should be observed.

The TREPR spectrum of **2**, namely an equimolar mixture of **3** and **6** dissolved in a toluene matrix, is virtually the superposition of two triplet EPR spectra (not shown). These are due to the porphyrin and the C_{60} triplet excited states, both carrying the typical spin polarization following ISC from the corresponding singlet excited precursors. The signal intensities of both triplets have similar grow-in dynamics, ruling out a possible energy-transfer process between the two moieties in the microsecond domain.

The TREPR spectrum of the same mixture (**3** and **6**) dissolved in THF (1×10^{-4} M) 1 μs after the laser pulse is shown in Figure 10 (180 K). The broad spectrum extends over about 4 mT, a much smaller spectral width than that observed in the toluene matrix (about 20 mT), and includes a much narrower component.

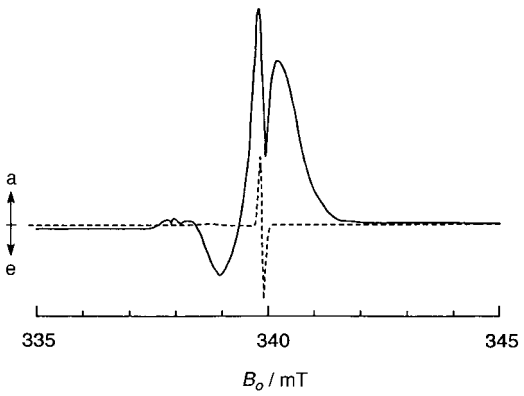

Figure 10. TREPR spectrum (solid line) observed 1 μs after the laser pulse excitation of dyad **2** dissolved in THF at 180 K. Positive and negative signals indicate absorptive (a) and emissive (e) polarizations. The broad TREPR spectrum was attributed to triplet-born ^{3}[Zn(tpp$^{\bullet+}$)($C_{60}^{\bullet-}$)] radical-ion pairs generated by intermolecular ET when partners of RPs are still close together (see later). The remaining narrow derivative-like a/e doublet was ascribed to a second ^{3}[Zn(tpp$^{\bullet+}$)($C_{60}^{\bullet-}$)] triplet-born RP state arising from intermolecular ET between unlinked [Zn(tpp)] and C_{60} molecules at larger distances (see later). Its calculated (dashed line) spectrum was obtained with zero mean dipolar contribution and positive spin exchange J constant of $+0.05$ mT. Linewidth of a/e doublet lines is $\delta B = 0.1$ mT. Microwave frequency: $\omega/2\pi = 9.5256$ GHz. Microwave field: $B_1 = 0.023$ mT. $2J$ is defined as the energy difference between the RP singlet state and the average value of the three zero-field levels of the RP triplet state.

The small spectral width of the two spectra in Figure 10 rules out the involvement of localized triplet excited states. Thus, in accordance with the optical results (see above) they are attributed to radical-ion pairs (RP) evolving from ET. The broad component of the spectrum should be noted, which carries an initial nonzero spin polarization, presumably an indication of the ^{3}*TPP state as its origin.

Radical ion pairs born in the triplet state have previously been reported that exhibit similar spectral features.[45] In the present case, the broad spectrum manifests a structure that is due to an electron–electron dipolar splitting. The separation between the outermost lines amounts to $2|D|$, where D denotes the dipolar coupling constant. Upon applying the classical expression of a point dipole model [Eq. (7)],[46] a

$$D/g\mu_B = 3/4\, g\mu_B(r^2 - 3z^2)/r^5 \approx -1.5\, g\mu_B/r^3 \quad (7)$$

center-to-center distance (r) between the cation and the anion of 11.7 Å is estimated from the measured $D/g\mu_B$ value (-1.72 mT). In this context, the calculated value of 9.5 Å for the center-to-center distance in the [Zn(tpp)C_{60}] complex should be considered. Thus, we assign the broad spectrum to a RP in which the cation and the anion radicals are slightly more weakly bound than in the complex. It would, however, represent a rather tightly bound RP in an uncomplexed form.

The spin-polarized EPR spectra of a mixture of **3** and **6** in THF, detected at different time delays after the laser pulse, are summarized in Figure 11. Initially a broad spectrum, consisting of four individual lines with an asymmetric shape and a partially emissive character at low fields, was detected. At longer times this transforms into a completely absorptive spin-polarization pattern of polarized lines.

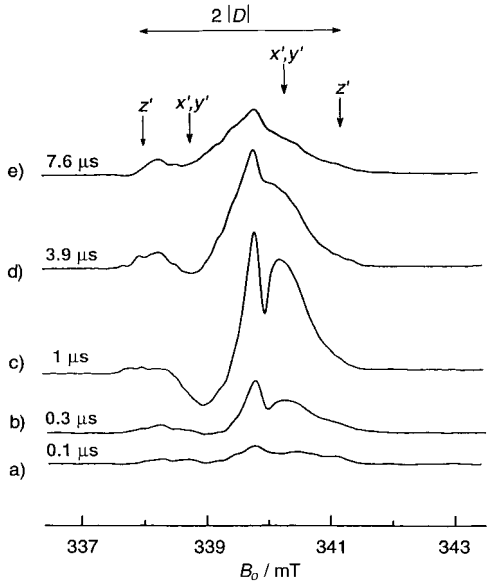

Figure 11. Spin-polarized EPR spectra of dyad **2** in THF detected at 180 K at different (indicated) delay times after the laser pulse. The turning points in the powder-like broad spectrum correspond to the canonical orientations $B_0 \| x'$, y', or z' for dipolar splittings in ^{3}[Zn(tpp$^{\bullet+}$)(C$_{60}^{\bullet-}$)]. As delay time increases, the early spectrum with partially emissive lines at low field evolves into a completely absorptive spectrum. Measured dipolar coupling constant $|D| = 1.72$ mT. Microwave frequency: $\omega/2\pi = 9.5256$ GHz. Microwave field: $B_1 = 0.023$ mT.

This time dependence can be explained in terms of a radical-pair mechanism,[47] in which the initial ET event from a triplet precursor is followed by an efficient singlet–triplet (S–T) mixing within the spin states of the RP. The overall mixing leads to a redistributing population among the triplet sublevels and hence a change in the spin polarization carried by the EPR spectra.

Figure 12 illustrates the sequence of processes, ET and S–T mixing with interconverting spin polarizations in the RP levels. Selective population of the ^{3}*TPP spin levels (reported in column "a" of Figure 12) is succeeded by a rapid ET, which essentially transfers population onto the RP spin levels that acquire an initial spin polarization. As a direct consequence, the triplet RP state shares its population with a nearly isoenergetic singlet state affording an S–T mixing.

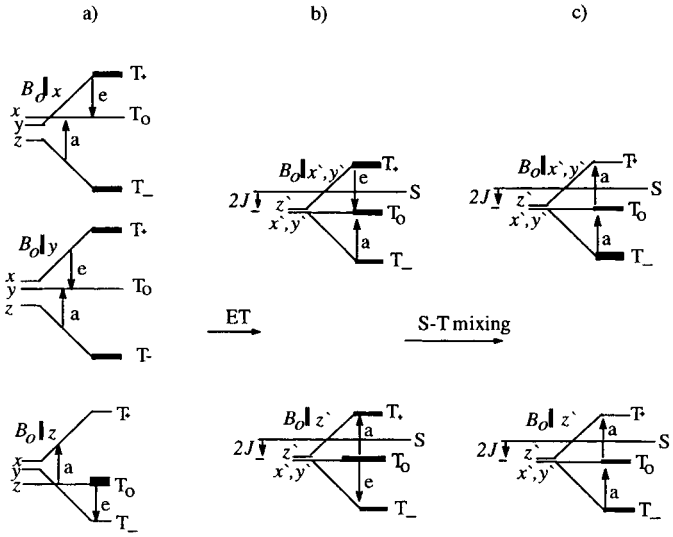

Figure 12. Zeeman energy levels and excess spin populations for the three canonical orientations of the triplet states ^{3}*[Zn(tpp)(C$_{60}$)] ($D > 0$) and ^{3}[Zn(tpp$^{\bullet+}$)(C$_{60}^{\bullet-}$)] ($D < 0$, $E = 0$). a) Initial high-field populations of ^{3}*[Zn(tpp)(C$_{60}$)] due to spin-selective ISC;[59] x,y,z are the principal axes of the ZFS tensor. b) Initial populations of ^{3}[Zn(tpp$^{\bullet+}$)(C$_{60}^{\bullet-}$)] caused by spin-polarization transfer from ^{3}*[Zn(tpp)(C$_{60}$)]. Assuming for RP the same structure as in the complex, the z' axis of the ZFS tensor of the RP lies along the line joining the centers of the porphyrin and C$_{60}$ moieties, and it is assumed, to a rough approximation, parallel to the z axis of the ZFS tensor of ^{3}*[Zn(tpp)(C$_{60}$)]. Therefore the whole polarization ($B_0 \| z$) of ^{3}[Zn(tpp)*(C$_{60}$)] is transferred to the z' orientation of ^{3}[Zn(tpp$^{\bullet+}$)(C$_{60}^{\bullet-}$)]. c) Qualitative description of the evolution of the populations of ^{3}[Zn(tpp$^{\bullet+}$)(C$_{60}^{\bullet-}$)] due to the different recombination rates of the triplet sublevels (S–T$_0$ and S–T$_+$ mixing) and spin relaxation.

In general, the spectral features of RPs depend on the sign of the spin exchange constant J defined as $2J = E(S) - E(T)$ (i.e., the difference in energy between the singlet and triplet states). Net emissive spectra have been observed in RPs in the presence of large negative J coupling.[47] Under these conditions, both S–T$_0$ and S–T$_-$ mixing are feasible and selective depopulation from these states affords, in accordance with their singlet character, a totally emissive EPR spectrum. This expectation is, however, in sharp contrast to the net absorptive spectrum reported in Figure 11. A positive J value is observed, as depicted in Figure 12, which is further accompanied by an efficient spin relaxation. The latter is capable of

0947-6539/01/0704-0824 $ 17.50+.50/0 Chem. Eur. J. 2001, 7, No. 4

restoring the populations between the T_0 and T_- spin states for the absorptive transition. As a final result a spin-polarization pattern in the triplet sublevels is established that yields a net absorption EPR spectrum, as shown in Figure 11. It is worth noting that in this case, $J > 0$ is a reasonable assumption. A recently published hypothesis suggests that the sign of the J constant in short-lived radical-ion pairs depends on the Marcus free energy. Accordingly, in a scenario in which the potential surfaces of the RP and ground states cross at the Marcus inverted region, a positive J is possible.[48]

To obtain more detailed information about the dynamics of the ET process we recorded the kinetic traces of the EPR signal for the magnetic field B_0 aligned with the principal axes x', y', and z' of the electron dipolar tensor of the RP triplet, as indicated in Figure 11. The traces of the low-field and high-field x' and y' peaks in the EPR spectrum were fitted by the same set of parameters,[47] and a triplet ET rate constant of $2 \times 10^6\ s^{-1}$ (at 180 K) was extracted from fitting the traces of Figure 13. From fitting the long-lived tails of the transient EPR signal an RP lifetime of 10 μs was estimated.

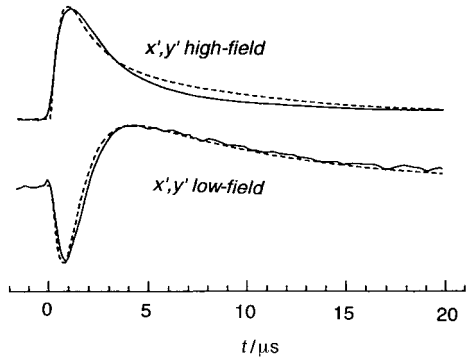

Figure 13. Kinetic traces of the low-field and high-field x',y' transitions of the EPR signals of ^{3}[Zn(tpp$^{\bullet+}$)($C_{60}^{\bullet-}$)] at 180 K. Positive signal indicates absorption and negative emission respectively. Both kinetic traces, corresponding to the transitions $T_+ \leftrightarrow T_0$ and $T_0 \leftrightarrow T_-$ in the RP spectra were fitted with the same set of rate constants by using the set of Equations (26) of ref. [59]. Extracted value for ET rate constant $k_{ET} = 2 \times 10^6\ s^{-1}$. Microwave field: $B_1 = 0.023$ mT.

In Figure 10, the central part of the spectrum shows a narrow derivative-like EPR signal with an antiphase a/e spin-polarization pattern (a and e being absorption and emission, respectively), which can be attributed to a spin correlated radical-ion pair (SCRP)[41, 49] that consists of the porphyrin π-radical cation and the fullerene π-radical anion. Recently, a similar spectrum was reported for a charge-separated state generated by intramolecular ET in a hydrogen-bonded porphyrindinitrobenzenezinc(II) complex.[50] The spin system is described as two unpaired electrons weakly coupled by a small spin exchange (J) and additional electron-electron dipolar (D) interactions. When the difference in the Zeeman energies for the two radicals is larger than the corresponding J and D constants, two doublets centered at the g factors of the two radicals in the SCRP are expected with an antiphase spin-polarization pattern.[41] In our case, the low-field doublet, centered at a g value of 2.0026 [Zn(tpp$^{\bullet+}$)],[50] is too broad to be detected because of its large linewidth, which is caused by unresolved hyperfine structure.[43] Thus, only the high-field doublet at a g value of 1.9998 ($C_{60}^{\bullet-}$) is detected. The best-fit simulation, shown in Figure 10, was obtained by allowing a zero anisotropic dipolar contribution to the spectrum and an isotropic $J/g\mu_B$ value of $+0.05$ mT (μ_B is the Bohr magneton). In this case the narrow spectrum width (0.1 mT) supports the view that the strength of dipolar interaction is markedly reduced, as in an uncomplexed or loosely bound RP, with respect to RP responsible for the broad spectrum. In fact, it gives rise to a negligible contribution to the $2[J - \{D(\cos^2\theta - 1/3)\}]$ splitting within the a/e doublet.[51] However, the effect cannot be ascribed solely to the averaging out of dipolar interaction caused by molecular tumbling because the same should be true for the broad spectrum where dipolar interaction is still visible.

Thus, the a/e doublet spectrum was attributed to the RP generated by ET between uncomplexed [Zn(tpp)] and C_{60}. Since the a/e spin-polarization pattern is compatible with either $J > 0$ and a triplet precursor or with $J < 0$ and a singlet precursor, the triplet excited state of the porphyrin was assumed to be the precursor state rather than the singlet one as previously proposed.[20] In fact, it is likely that in the uncomplexed form, the singlet excited state of the porphyrin molecule has enough time to convert into the corresponding triplet excited state before ET can take place. We note that the common origin of the RPs is supported by the fact that a positive J value was used in the simulation of both species. This, of course, was done with the assumption that for radical-ion pairs an inversion in the relative position of triplet and singlet energy levels is feasible.[48]

EPR results obtained for the RPs in THF necessitate two final comments. First, the EPR experiments undoubtedly reveal the presence of RPs generated from a triplet precursor in which the two partners of the RP remain at an average distance of 11.7 Å from each other. It is feasible that stabilization of the latter is gained by Coulombic attraction.[52] Secondly, according to the SCRP theory[41, 49] the narrow EPR spectrum, characterized by an antiphase spin polarization (see Figure 10) and assigned to another unlinked RP, provides evidence that the two ions, held together at an even larger distance, preserve their spin correlation during the time window (microseconds) open for EPR experiment.

In our case two microscopic structures formed by pairs of negatively and positively charged ions at increasingly larger distances are stabilized in the fluid phase. Therefore, even at large distances, a stable structure of the radicals in the separated RP is sustained, characterized by an equilibrium distance and a corresponding binding energy. These results are supported by the observation of long-lived radical pairs formed by acetone ketyl radicals in alcohols at low temperature (−70 °C).[53] However, in general, attention should be paid to the presence of long-lived radical pairs in fluids. In fact, recently, the origin of the antiphase structure (APS) observed in the transient EPR spectra of short-lived RPs in micelles[49] or other confined environments and even in liquids[53] has been questioned, and an alternative mechanism for APS production has been proposed.[54] In this model the presence of APS is also expected for freely diffusing pairs of radicals and the lifetime of APS is determined by the lifetime of the radicals or by the relaxation time.

Conclusion

In conclusion, we have shown that the complexation of a pyridine-fullerene derivative to a [Ru(tpp)(CO)] unit produces a relatively stable dyad complex that gives rise to primarily intramolecular energy transfer from the photoexcited porphyrin to the fullerene in toluene. To a small extent intramolecular charge-separated states are observed in a more polar solvent like benzonitrile. However, these recombine rapidly. More interestingly, complexation of a pyridine-fullerene derivative to a [Zn(tpp)] complex is reversible and gives rise to very efficient charge separation upon irradiation. In a polar solvent intra- and intermolecular ET generate charge-separated states with radical-ion pairs that have lifetimes of about 10 μs (in THF) and several hundreds of microseconds (in benzonitrile). EPR spectra provide evidence that two long-lived radical-ion pairs with comparable lifetimes exist in THF and are characterized by a different mean distance between charged radicals. We are currently using structurally different fullerene-pyridine derivatives to investigate the influence of the geometry of the complex on the photoinduced processes. On the other hand, the example reported here demonstrates the potential utility of these noncovalently linked systems in photovoltaic devices. The lifetime of the charge-separated species is in fact long enough to envision utilization of the relative chemical energy. Work along these lines is underway.

Experimental Section

General: Details regarding instrumentation used in this paper have been described elsewhere.[55] Compound **3** was prepared according to our previous report.[25] All other reagents were used as purchased from Fluka and Aldrich.

Synthesis of complex 1: Solutions of **3** (54.3 mg, 0.063 mmol) and **4** (approximately 50.5 mg, 0.063 mmol) in chloroform were combined under stirring. After 30 minutes the solvent was evaporated, the residue was dissolved in methylene chloride, and the product was precipitated by addition of methanol, yielding 91.5 mg (90 %). ^{1}H NMR (200 MHz, $CDCl_3$): $\delta = 8.55$ (m, 8H), 8.21 (m, 4H), 7.86 (m, 4H), 7.70 (m, 8H), 7.59 (m, 4H), 5.80 (m, 2H), 4.47 (d, $J = 9.5$ Hz, 1H), 3.79 (s, 1H), 3.71 (d, $J = 9.5$ Hz, 1H), 1.94 (s, 3H), 1.59 (m, 2H); ^{13}C NMR (50 MHz, $CDCl_3$): $\delta =$ 179.8, 155.1, 152.9, 151.2, 150.6, 147.3, 146.3, 146.2, 146.1, 146.1, 145.9, 145.9, 145.4, 145.3, 145.2, 145.2, 145.0, 144.6, 144.3, 144.3, 144.2, 143.7, 143.4, 143.4, 143.1, 142.8, 142.7, 142.6, 142.6, 142.5, 142.0, 142.0, 141.9, 141.8, 141.6, 141.5, 141.3, 141.0, 140.0, 140.0, 139.3, 139.3, 135.9, 135.2, 134.2, 134.0, 131.8, 127.2, 126.5, 126.2, 121.8, 121.7, 80.3, 75.4, 69.3, 68.4, 39.1; IR (NaCl): $\tilde{\nu} = 3564$, 3457, 3018, 2778, 1962, 1596, 1438, 1350, 1176, 1072, 1006, 751, 702, 526 cm^{-1}; ES-MS (THF/MeOH 1:1): m/z: 855 $[M+H]^+$; elemental analysis calcd (%) for $C_{113}H_{38}N_6O$ Ru: C 85.01, H 2.40, N 5.26; found C 84.38, H 2.38, N 5.24.

Association constant measurement: Solutions of [Zn(tpp)] (**6**) were mixed with appropriate amounts of a solution of fulleropyrrolidine (**3**, 3×10^{-4} M in toluene) in order to achieve a final [Zn(tpp)] (**6**) concentration of 1×10^{-5} M and relative ratios **3**:**6** of 1.4, 2.7, 3.9, 5.0, 6.0, 6.9, 7.7, 8.6, 9.3, and 10.0 (Figure 2 bottom). The reference cuvette in the spectrophotometer contained the exact concentration of fullerene present in the sample cuvette. The binding isotherm was obtained by plotting the absorbance at 550 nm against the concentration of **3** and the results were fitted using the program HOSTEST II.[56]

Laser flash photolysis: Picosecond laser flash photolysis experiments were carried out with 532 nm laser pulses from a mode-locked, *Q*-switched Quantel YG-501 DP Nd:YAG laser system (pulse width 18 ps, 2–3 mJ/pulse). Passing the fundamental output through D_2O/H_2O generated the white continuum picosecond probe pulse. The excitation and the probe were fed to a spectrograph (HR-320, ISDA Instruments) with fiberoptic cables and were analyzed with a dual diode array detector (Princeton Instruments) interfaced with an IBM-AT computer. Nanosecond laser flash photolysis was performed with laser pulses from a Quanta-Ray CDR Nd:YAG system (532 nm, 6 ns pulse width, 5–10 mJ per pulse) in a front-face excitation geometry. The photomultiplier output was digitized with a Tektronix 7912 AD programmable digitizer. A typical experiment consisted of 5–10 replicate pulses per measurement. The averaged signal was processed with a LSI-11 microprocessor interfaced with a VAX-370 computer. The details of the experimental set ups and their operation have been described elsewhere.[57]

Pulse radiolysis: Pulse radiolysis experiments were performed by utilizing 50 ns pulses of 8 MeV electrons from a Model TB-8/16-1S electron linear accelerator. Basic details of the equipment and the data analysis have been described elsewhere.[59] Dosimetry was based on the oxidation of SCN^- to $(SCN)_2^{\bullet -}$, which in aqueous N_2O-saturated solutions takes place with $G = 6$ (G denotes the number of species per 100 eV, or the approximate micromolar concentration per 10 J of absorbed energy). The radical concentration generated per pulse amounts to $(1-3) \times 10^{-6}$ M for all of the systems investigated in this study.

EPR spectroscopy: Transient EPR measurements were carried out by using a Bruker ER 200D X-band EPR spectrometer, equipped with a fast microwave preamplifier and a broad band video amplifier (band width 100 Hz–6.5 MHz) CW-TREPR, in direct detection (DD) mode with interface to a pulsed dye laser. The sample was irradiated at a repetition rate of 20 Hz by a Lambda Physik LPX 100 XeCl excimer laser coupled to a modified FL 200 dye laser using Rhodamin 6G dye laser (pulse width 8 ns, energy per pulse ~5 mJ). Light emitted at 580 nm was conveyed into a rectangular standard TE_{102} microwave cavity with optical access. The response time of the EPR detection was 150 ns. The temperature was controlled by a variable-temperature nitrogen flow dewar inside the EPR resonator. The EPR spectrum was obtained by following the signal generated by the laser light as output of a boxcar integrator (EG&EG equipped with 162 plug-in), while sweeping the magnetic field under constant microwave irradiation. A time window of 50 ns was used at a fixed delay of 0.5 s from the laser pulse. A transient recorder (LeCroy 9450A) digitized traces of the transient EPR signal, a fast digital oscilloscope operating at maximum acquisition rate of 400 megasamples s^{-1} synchronized with the laser pulse. Data collection was controlled by a personal computer, which allowed control of the magnetic field, the setting of the digital oscilloscope, and data acquisition. At each magnetic field value typically 300 transient signals containing 400 points each were averaged and stored in the computer memory before stepping to the next field value. The field sweep was performed in 128 steps. The 400×128 matrix gave a two-dimensional surface (time-field) spectrum, from which either a field-swept spectrum or a transient signal was extracted.

Acknowledgement

We are grateful to Professors Paolo Scrimin and Paolo Tecilla for help in the calculation of the binding constant between **3** and **6**. This work was supported in part by the Office of Basic Energy Sciences of the U.S. Dept. of Energy, by MURST (cofin. ex 40 %, prot. n. mm319 8284) and by C.N.R. through the program "Materiali Innovativi (legge 95/95)". This is contribution No. NDRL-4243 from the Notre Dame Radiation Laboratory.

[1] B. A. Heller, D. Holten, C. Kirmaier, *Science* **1995**, *269*, 940.
[2] N. R. S. Reddy, S. V. Kolaczkowski, G. J. Small, *Science* **1993**, *260*, 68.
[3] *Carotenoids Photosynthesis* (Eds.: A. J. Young, G. Britton), Chapmann and Hall, London (UK), **1993**.
[4] T. J. Meyer, *Acc. Chem. Res.* **1989**, *22*, 163.
[5] M. R. Wasielewski, *Chem. Rev.* **1992**, *92*, 435.
[6] D. Gust, T. A. Moore, A. L. Moore, *Acc. Chem. Res.* **1993**, *26*, 198.
[7] A. J. Bard, M. A. Fox, *Acc. Chem. Res.* **1995**, *28*, 141.
[8] H. Kurreck, M. Huber, *Angew. Chem.* **1995**, *107*, 929; *Angew. Chem. Int. Ed. Engl.* **1995**, *34*, 849.

[9] J. L. Sessler, B. Wang, S. L. Springs, C. T. Brown in *Comprehensive Supramolecular Chemistry*, Pergamon, Oxford (UK), **1996**, 311.
[10] T. Hayashi, H. Ogoshi, *Chem. Soc. Rev.* **1997**, *26*, 355.
[11] M. D. Ward, *Chem. Soc. Rev.* **1997**, *26*, 365.
[12] a) S. Springs, D. Gosztola, M. Wasielewski, V. Král, A. Andrievsky, J. Sessler, *J. Am. Chem. Soc.* **1999**, *121*, 2281; b) K. Yamada, H. Imahori, E. Yoshizawa, D. Gosztola, M. Wasielewski, Y. Sakata, *Chem. Lett.* **1999**, 235; c) C. Hunter, J. Sanders, G. Beddard, S. Evans, *J. Chem. Soc. Chem. Commun.* **1989**, 1765; d) H. Anderson, C. Hunter, J. Sanders, *J. Chem. Soc. Chem. Commun.* **1989**, 226.
[13] H. Imahori, Y. Sakata, *Adv. Mater.* **1997**, *9*, 537.
[14] H. Imahori, Y. Sakata, *Eur. J. Org. Chem.* **1999**, 2445.
[15] D. M. Guldi, *Chem. Commun.* **2000**, 321.
[16] M. Prato, *J. Mater. Chem.* **1997**, *7*, 1097.
[17] M. Prato, *Top. Curr. Chem.* **1999**, *199*, 173.
[18] H. Imahori, K. Hagiwara, M. Aoki, T. Akiyama, S. Taniguchi, T. Okada, M. Shirakawa, Y. Sakata, *Chem. Phys. Lett.* **1996**, *263*, 545.
[19] D. M. Guldi, K.-D. Asmus, *J. Am. Chem. Soc.* **1997**, *119*, 5744.
[20] T. Da Ros, M. Prato, D. Guldi, E. Alessio, M. Ruzzi, L. Pasimeni, *Chem. Commun.* **1999**, 635.
[21] N. Armaroli, F. Diederich, L. Echegoyen, T. Habicher, L. Flamigni, G. Marconi, J.-F. Nierengarten, *New J. Chem.* **1999**, 77.
[22] F. D'Souza, G. R. Deviprasad, M. S. Rahman, J.-P. Choi, *Inorg. Chem.* **1999**, *38*, 2157.
[23] M. Maggini, G. Scorrano, M. Prato, *J. Am. Chem. Soc.* **1993**, *115*, 9798.
[24] M. Prato, M. Maggini, *Acc. Chem. Res.* **1998**, *31*, 519.
[25] M. Prato, M. Maggini, C. Giacometti, G. Scorrano, G. Sandonà, G. Farnia, *Tetrahedron* **1996**, *52*, 5221.
[26] J. Bonnet, S. Eaton, G. Eaton, R. Holm, J. Ibers, *J. Am. Chem. Soc.* **1973**, *95*, 2141.
[27] C. Kirskey, P. Hambright, C. Storm, *Inorg. Chem.* **1969**, *8*, 2141.
[28] J. Rodriguez, C. Kirmaier, D. Holten, *J. Am. Chem. Soc.* **1989**, *111*, 6500.
[29] A. Weller, *Z. Physik. Chem.* **1982**, *132*, 93.
[30] C. D. Tait, D. Holten, M. H. Barley, D. Dolphin, B. R. James, *J. Am. Chem. Soc.* **1985**, *107*, 1930.
[31] D. M. Guldi, M. Maggini, G. Scorrano, M. Prato, *J. Am. Chem. Soc.* **1997**, *119*, 974.
[32] N. E. Shank, L. M. Dorfman, *J. Chem. Phys.* **1970**, *52*, 4441.
[33] D. M. Guldi, P. Neta, P. Hambright, D. Lexa, J.-M. Saveant, *J. Phys. Chem.* **1992**, *96*, 4459.
[34] G. L. I. Gaines, M. P. O'Neil, W. A. Svec, M. P. Niemczyk, M. R. Wasielewski, *J. Am. Chem. Soc.* **1991**, *113*, 719.
[35] D. M. Guldi, K.-D. Asmus, *J. Phys. Chem.* **1997**, *101*, 1472.
[36] P. A. Liddell, J. P. Sumida, A. N. Macpherson, L. Noss, G. R. Seely, K. N. Clark, A. L. Moore, T. A. Moore, D. Gust, *Photochem. Photobiol.* **1994**, *60*, 537.
[37] D. Kuciauskas, S. Lin, G. R. Seely, A. L. Moore, T. A. Moore, D. Gust, T. Drovetskaya, C. A. Reed, P. D. W. Boyd, *J. Phys. Chem.* **1996**, *100*, 15926.
[38] S. S. Eaton, G. R. Eaton, R. H. Holm, *J. Organometal. Chem.* **1972**, *39*, 179.
[39] G. Agostini, C. Corvaja, L. Pasimeni, *Chem. Phys.* **1996**, *202*, 349.
[40] M. R. Wasielewski, M. P. O'Neill, K. R. Lykke, M. J. Pellin, D. M. Gruen, *J. Am. Chem. Soc.* **1991**, *113*, 2774.
[41] C. D. Buckley, D. A. Hunter, P. J. Hore, K. A. McLauchlan, *Chem. Phys. Lett.* **1987**, *135*, 307.
[42] J. R. Norris, A. L. Morris, M. C. Thurnauer, J. Tang, *J. Chem. Phys.* **1990**, *92*, 4239.
[43] J. Fajer, D. C. Borg, A. Forman, D. Dolphin, R. H. Felton, *J. Am. Chem. Soc.* **1970**, *92*, 3451.
[44] S. L. Murov, I. Carmichael, G. L. Hug, *Handbook of Photochemistry*, Marcel Dekker, New York, **1993**.
[45] N. I. Avdievich, K. E. Dukes, M. D. E. Forbes, J. M. D. Simone, *J. Phys. Chem. A* **1997**, *101*, 617.
[46] A. Carrington, A. D. McLachlan, *Introduction to Magnetic Resonance*, Harper and Row, London (UK), **1967**.
[47] J. Schlüpmann, F. Lendzian, M. Plato, K. Möbius, *J. Chem. Soc. Faraday Trans.* **1993**, *89*, 2853.
[48] S. Sekiguchi, Y. Kobori, K. Akiyama, S. Tero-Kubota, *J. Am. Chem. Soc.* **1998**, *120*, 1325.
[49] G. L. Closs, M. D. E. Forbes, J. R. Norris, *J. Phys. Chem.* **1987**, *91*, 3592.
[50] M. Asano-Someda, H. Levanon, J. L. Sessler, R. Wang, *Mol. Phys.* **1998**, *95*, 935.
[51] P. J. Hore in *Advanced EPR. Applications in Biology and Biochemistry*, Elsevier, Amsterdam, **1989**, 405.
[52] G. Kroll, M. Pluschau, K.-P. Dinse, H. v. Willigen, *J. Chem. Phys.* **1990**, *93*, 8709.
[53] K. Tominaga, S. Yamauchi, N. Hirota, *J. Chem. Phys.* **1990**, *92*, 5175.
[54] A. A. Neufeld, J. B. Pedersen, *J. Chem. Phys.* **1998**, *109*, 8743.
[55] T. Da Ros, M. Prato, F. Novello, M. Maggini, E. Banfi, *J. Org. Chem.* **1996**, *61*, 9070.
[56] C. S. Wilcox in *Frontiers in Supramolecular Organic Chemistry and Photochemistry* (Eds.: H.-J. Schneider, H. Dürr), VCH, Weinheim, **1991**.
[57] M. D. Thomas, G. L. Hug, *Comput. Chem.* **1998**, *22*, 491.
[58] G. L. Hug, Y. Wang, C. Schöneich, P.-Y. Jiang, R. W. Fessenden, *Radiat. Phys. Chem.* **1999**, *54*, 559.
[59] J. Schlüpmann, K. M. Salikhov, M. Plato, P. Jägermann, F. Lendzian, K. M*öbius*, *Appl. Magn. Res.* **1991**, *2*, 117.

Received: May 9, 2000 [F2477]